

A predictive model to guide management of the overlap region between target volume and organs at risk in prostate cancer volumetric modulated arc therapy

Malcolm D. Mattes, MD, Jennifer C. Lee, BS, Sara Elnaiem, BS,
Adel Guirguis, MD, N. C. Ikoro, PhD, Hani Ashamalla, MD

Department of Radiation Oncology, New York Methodist Hospital, Brooklyn, NY, USA

Purpose: The goal of this study is to determine whether the magnitude of overlap between planning target volume (PTV) and rectum (Rectum_{overlap}) or PTV and bladder (Bladder_{overlap}) in prostate cancer volumetric-modulated arc therapy (VMAT) is predictive of the dose-volume relationships achieved after optimization, and to identify predictive equations and cutoff values using these overlap volumes beyond which the Quantitative Analyses of Normal Tissue Effects in the Clinic (QUANTEC) dose-volume constraints are unlikely to be met.

Materials and Methods: Fifty-seven patients with prostate cancer underwent VMAT planning using identical optimization conditions and normalization. The PTV (for the 50.4 Gy primary plan and 30.6 Gy boost plan) included 5 to 10 mm margins around the prostate and seminal vesicles. Pearson correlations, linear regression analyses, and receiver operating characteristic (ROC) curves were used to correlate the percentage overlap with dose-volume parameters.

Results: The percentage Rectum_{overlap} and Bladder_{overlap} correlated with sparing of that organ but minimally impacted other dose-volume parameters, predicted the primary plan rectum V₄₅ and bladder V₅₀ with R² = 0.78 and R² = 0.83, respectively, and predicted the boost plan rectum V₃₀ and bladder V₃₀ with R² = 0.53 and R² = 0.81, respectively. The optimal cutoff value of boost Rectum_{overlap} to predict rectum V₇₅ >15% was 3.5% (sensitivity 100%, specificity 94%, p < 0.01), and the optimal cutoff value of boost Bladder_{overlap} to predict bladder V₈₀ >10% was 5.0% (sensitivity 83%, specificity 100%, p < 0.01).

Conclusion: The degree of overlap between PTV and bladder or rectum can be used to accurately guide physicians on the use of interventions to limit the extent of the overlap region prior to optimization.

Keywords: Prostate cancers, Organs at risk, Radiation injuries, Computer assisted radiotherapy planning, Intensity-modulated radiotherapy

Introduction

Intensity-modulated radiation therapy (IMRT) is an inverse treatment planning process that optimizes the intensity distribution of a set of beams according to dose-volume histogram objectives chosen by planners, allowing for highly

conformal treatment of a target while sparing organs-at-risk (OARs). IMRT has been shown to be particularly valuable compared to three-dimensional conformal radiation therapy (3D-CRT) when there is a significant overlap between the planning target volume (PTV) and an OAR [1-3]. Volumetric-modulated arc therapy (VMAT), the next generation of IMRT,

Received 6 September 2013, Revised 20 December 2013, Accepted 16 January 2014.

Correspondence: Malcolm D. Mattes, MD, Department of Radiation Oncology, New York Methodist Hospital, 506 6th St, Brooklyn, NY 11215, USA. Tel: +1-718-780-3677, Fax: +1-718-780-3688, E-mail: mdm9007@nyp.org

© This is an Open Access article distributed under the terms of the Creative Commons Attribution Non-Commercial License (<http://creativecommons.org/licenses/by-nc/3.0/>) which permits unrestricted non-commercial use, distribution, and reproduction in any medium, provided the original work is properly cited.

www.e-roj.org

allows for variation in the dose rate, speed of gantry rotation, and multi-leaf positions during rotation of the gantry in a full 360 degree arc, and has been shown to yield even further OAR sparing as compared to fixed-beam IMRT in prostate cancer [4,5]. However, regardless of the treatment delivery technique, if a large amount of overlap between PTV and OAR exist it may be physically impossible to achieve uniform coverage of the PTV with the prescription dose while also adequately sparing that OAR [6].

In prostate cancer radiotherapy, the PTV frequently overlaps the bladder and rectum with the degree of overlap dependent on patient anatomy, contouring technique (i.e., the way the prostate, bladder, and rectum are defined during treatment planning) and the PTV expansion used. While the overlap region generally makes up only a small percentage of the PTV, it is an important area to adequately treat given that most prostate cancer develops in the peripheral zone of the prostate [7,8]. Attempts have been made to spare patients some morbidity by excluding the OAR from PTV or intentionally under-dosing the overlap region [9,10], though the consequences of such techniques on tumor control probability are difficult to estimate.

In recent years, mathematical algorithms based on machine learning have been developed for head and neck cancer and prostate cancer fixed-beam IMRT through which planners can use the geometric relationship of the PTV and OAR to quantify and predict the achievable OAR sparing for an individual patient based on prior experiences from plans generated in previous patients [11,12]. The use of such modeling is somewhat limited in the sense that it is based on plans with the same features (i.e., beam configuration, beam energy, number of beams, etc.), and thus may be less accurate if any of these factors are changed for instance in VMAT, tomotherapy, or particle therapy. Nonetheless, these techniques have been used to streamline the treatment planning process and as a metric of quality control in IMRT planning [13]. Another issue is that while they provide ways in which a given overlap volume can be managed from a treatment planning perspective, they do not necessarily give the physician information on when it would be justifiable to take additional measures to reduce the overlap volume prior to optimization. Such measures in prostate cancer may include cytoreduction with androgen-deprivation therapy [14], the use of daily cone-beam computed tomography (CT) or implantable fiducials to safely reduce PTV margins through improved target localization [15-17], or the use of spacer gel injection between

the prostate and rectum [18-20].

The goal of this project is to aid physicians in determining when interventions to reduce the overlap volume prior to treatment planning are most applicable to their patients, by quantitatively determining predictive equations and cutoff values for the overlap volume between the PTV and rectum ($\text{Rectum}_{\text{overlap}}$) or PTV and bladder ($\text{Bladder}_{\text{overlap}}$) above which the Quantitative Analyses of Normal Tissue Effects in the Clinic (QUANTEC) dose-volume constraints for these organs are unlikely to be achieved. A secondary objective was to determine whether the degree of overlap between PTV and OAR affects other aspects of plan quality besides the dose to that OAR, for instance the dose to other OARs, integral dose, conformity to the PTV or dose gradient. This study also represents an extension of overlap analysis to VMAT, as has not been undertaken in the previous IMRT studies. In this way, we sought to develop a front-end approach to managing the overlap region to complement the optimization algorithms described above.

Materials and Methods

Fifty-seven consecutive patients with low risk prostate cancer (T1c-T2a, Gleason score <6, prostate-specific antigen <10) treated at our institution from 2011 to 2012 underwent CT simulation in the supine position with urethrogram. A target volume encompassing the prostate and entire seminal vesicles was prescribed to 50.4 Gy in 1.8 Gy fractions (primary plan), to be followed by a 30.6 Gy boost in 1.8 Gy fractions to the prostate and proximal seminal vesicles (boost plan), to a total dose of 81 Gy (summation plan). None of the target volumes included the whole pelvis or pelvic lymph nodes. The PTV for the primary plan included a 10-mm margin around the clinical target volume laterally, a 7-mm margin anteriorly and posteriorly, and a 7-mm superiorly and inferiorly, whereas the PTV for the boost plan included a 7-mm margin laterally and a 5-mm margin in all other directions. Rectal outer contours were outlined from the level of the ischial tuberosities to the level of the inferior border of the sacroiliac joints. The PTV, bladder, rectum, and femoral heads were delineated for each patient at the discretion of a single experienced radiation oncologist. VMAT plans were generated using 6 MV photons and two full arcs for the Varian iX linear accelerator (Varian Medical Systems, Palo Alto, CA, USA) using the Eclipse system (ver. 8.6) and identical optimization conditions as shown in Table 1. These optimization conditions for the primary and

boost plans were chosen to be consistent with the clinical dose-volume constraints for a full course of prostate IMRT represented in the QUANTEC guidelines [21]. The analytical anisotropic algorithm was used for all dose calculations [22]. In our practice, VMAT is used for both the primary plan and the boost plan. All plans were normalized such that 98% of the PTV received 100% of the prescribed dose. All treatment plans involved in this study were generated exclusively for the purpose of this study, and were not used for the actual treatment of patients.

Percentage overlap was defined as the volume of overlap between a given PTV and OAR divided by the total volume of that OAR. V_x was defined as the volume of the OAR receiving more than dose x (Gy). The maximum and minimum doses to the PTV were defined as the highest and lowest dose, respectively, within 0.03 mL of the PTV. The normal tissue integral dose was calculated as the product of the mean dose to a region encompassing the normal tissue (excluding the PTV) inside the scanned region, and the volume of that region. The conformity index was calculated as (volume within the prescription isodose surface) / (volume of the PTV that is enclosed by the prescription isodose line), with a value closer to unity indicating greater conformity. The gradient measure was the difference in centimeters between the equivalent sphere radii of the prescription and half prescription isodose lines. A smaller gradient measure indicates higher dose gradients around the target.

Table 1. Optimization conditions for primary plan and boost plan

	Primary plan (50.4 Gy)			Boost plan (30.6 Gy)		
	Dose (Gy)	Volume (%)	Priority (%)	Dose (Gy)	Volume (%)	Priority (%)
PTV	48	>99.9	70	29	>99.9	70
	53	<0.1	70	32	<0.1	70
Bladder	20	<70	30	10	<70	30
	35	<40	40	20	<40	40
	50	<10	50	30	<10	50
Rectum	15	<70	30	10	<65	30
	30	<40	40	20	<35	40
	45	<10	50	30	<5	50
	50	<3	60	-	-	-
Femoral heads	15	<50	10	10	<50	10
	30	<2	20	20	<2	20
Body	54	<0.01	80	33	<0.01	80

A high priority value means greater importance will be attached to achieving that particular dose constraint.

PTV, planning target volume.

The 57 patient cohort included in this study was divided according to chronology into a 29 patient training set and a separate 28 patient validation set. Using the training set, Pearson product-moment correlations were used to determine any associations between dose-volumetric parameters and the percentage overlap between the PTV and the rectum ($Rectum_{overlap}$) or PTV and the bladder ($Bladder_{overlap}$) [23]. Dose-volumetric parameters evaluated for the primary plans included bladder V_{50} , V_{35} , & V_{20} , rectum V_{45} , V_{30} , & V_{15} , mean dose to the femoral heads (femoral heads D_{mean}), maximum dose to the PTV ($PTV D_{max}$), minimum dose to the PTV ($PTV D_{min}$), normal tissue integral dose (NTID), conformity index (CI), gradient measure (GM), and monitor units (MUs). Dose-volumetric parameters evaluated for the boost plans included bladder V_{30} , V_{20} , & V_{10} , rectum V_{30} , V_{20} , & V_{10} , femoral heads D_{mean} , $PTV D_{max}$, $PTV D_{min}$, NTID, CI, GM, and MUs. Linear regression analyses were carried out on the training set for the primary and boost plans to determine predictive formulas for the high-dose region OAR constraints using the percentage $Rectum_{overlap}$ and $Bladder_{overlap}$. Statistical comparison of the average sum of residuals (SR_{rectum} and $SR_{bladder}$) between training and validation cohorts was used to quantify the accuracy of the regression models. Receiver operating characteristic (ROC)

Table 2. Pearson product-moment correlations (r) associating the percentage overlap between the PTV and OARs ($Rectum_{overlap}$ and $Bladder_{overlap}$ respectively) with dose-volumetric parameters for the primary plans

	$Rectum_{overlap}$		$Bladder_{overlap}$	
	r	p-value	r	p-value
Bladder				
V_{20}	-0.098	0.54	0.595	<0.01
V_{35}	-0.121	0.45	0.746	<0.01
V_{50}	-0.072	0.65	0.911	<0.01
Rectum				
V_{15}	0.437	<0.01	-0.066	0.68
V_{30}	0.588	<0.01	-0.025	0.87
V_{45}	0.883	<0.01	-0.110	0.49
Femoral heads D_{mean}	0.169	0.30	0.013	0.94
PTV				
D_{min}	-0.068	0.67	-0.207	0.19
D_{max}	0.309	0.05	0.203	0.20
Integral dose	-0.041	0.79	-0.073	0.65
Conformity index	0.419	0.01	-0.094	0.55
Gradient measure	0.148	0.35	-0.056	0.73
Monitor units	0.110	0.49	-0.036	0.82

PTV, planning target volume; OARs, organs-at-risk.

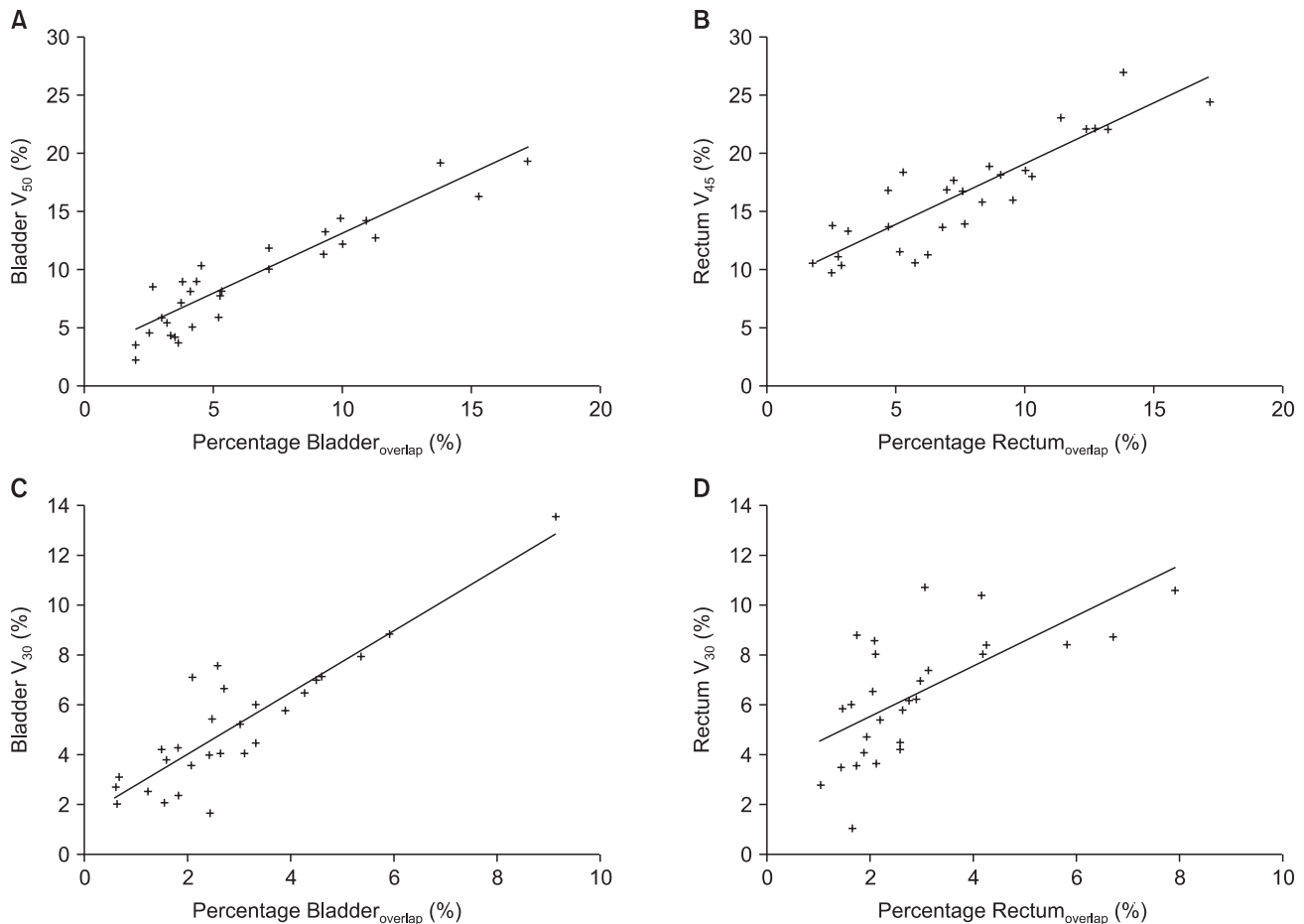


Fig. 1. Linear regression analysis using the percentage overlap between the planning target volume and organs-at-risk to predict the Bladder V_{50} and Rectum V_{45} for the primary plan (A, B) and Bladder V_{30} and Rectum V_{30} boost plan (C, D).

curves were applied to the summation plans to determine if the boost plan percentage $\text{Rectum}_{\text{overlap}}$ and $\text{Bladder}_{\text{overlap}}$ could predict generation of a plan that deviated from the QUANTEC high-dose-region constraints of $\text{Rectum } V_{75} < 15\%$ and $\text{Bladder } V_{80} < 15\%$. The cutoff values generated by this method were applied to the validation set to determine their performance in classifying whether plans would meet these constraints. Statistical analysis was performed using Statistical Package for Social Sciences 20.0 (IBM Corporation, Chicago, IL, USA) and Microsoft Excel 2007 (Microsoft Corporation, Redmond, WA, USA). A p-value less than 0.05 was considered statistically significant.

Results

For the primary plan, the median $\text{Rectum}_{\text{overlap}}$ for the entire cohort of patients was 3.58 cm^3 (range, 0.62 to 16.68 cm^3), or 6.52% of the median rectum volume (range, 0.84% to 17.08%).

The median $\text{Bladder}_{\text{overlap}}$ was 5.91 cm^3 (range, 1.08 to 23.94 cm^3), or 4.68% of the median bladder volume (range, 1.48% to 17.16%). The median percentage $\text{Rectum}_{\text{overlap}}$ of the training set was 6.87% (range, 1.36% to 17.08%), whereas that of the validation set was 6.37% (range, 0.84% to 13.11%). The median percentage $\text{Bladder}_{\text{overlap}}$ of the training set was 4.53% (range, 1.65% to 17.16%), whereas that of the validation set was 5.30% (range, 1.48% to 16.22%). Neither of these differences were statistically significant ($p = 0.71$ and $p = 0.58$, respectively). Pearson correlations between the primary plan $\text{Rectum}_{\text{overlap}}$ or $\text{Bladder}_{\text{overlap}}$ and dose-volumetric parameters are shown in Table 2. Of the parameters tested, there were statistically significant associations between $\text{Rectum}_{\text{overlap}}$ and $\text{Rectum } V_{45}$ ($r = 0.883$, $p < 0.01$), V_{30} ($r = 0.588$, $p < 0.01$) and V_{15} ($r = 0.437$, $p < 0.01$), and CI ($r = 0.419$, $p = 0.01$). There were also statistically significant associations between $\text{Bladder}_{\text{overlap}}$ and $\text{Bladder } V_{50}$ ($r = 0.911$, $p < 0.01$), V_{35} ($r = 0.746$, $p < 0.01$), and V_{20} ($r = 0.595$, $p < 0.01$). On linear regression analysis (Fig. 1A, B),

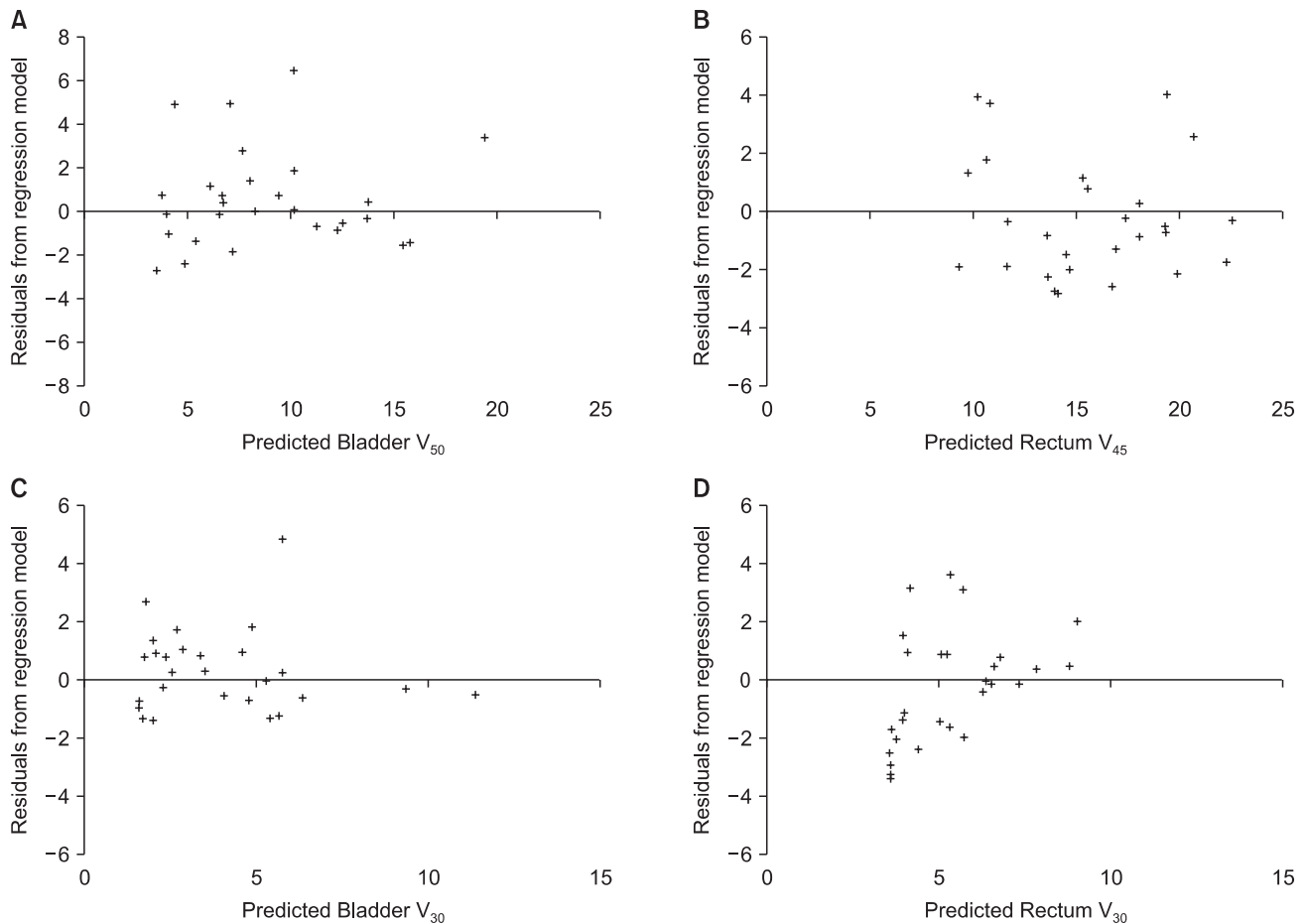


Fig. 2. Residual values for the validation set using the linear regression models generated to predict the Bladder V_{50} and Rectum V_{45} for the primary plan (A, B) and Bladder V_{30} and Rectum V_{30} boost plan (C, D).

the equation $[1.05 \times (\text{percentage Rectum}_{\text{overlap}}) + 8.79]$ predicts Rectum V_{45} with an R^2 of 0.78 ($p < 0.01$), and the equation $[1.02 \times (\text{percentage Bladder}_{\text{overlap}}) + 2.91]$ predicts Bladder V_{50} with an R^2 of 0.83 ($p < 0.01$), indicating that the full models accounts for 78% and 83% of data variability, respectively. The predictive abilities of the regression models for the primary plan were statistically indistinguishable between the training and validation sets, with $SR_{\text{Rectum}} = -0.31 \pm 2.03$ and $SR_{\text{Bladder}} = 0.56 \pm 2.24$ for the validation set (Fig. 2A, B).

For the boost plan, the median $\text{Rectum}_{\text{overlap}}$ for the entire cohort of patients was 1.18 cm^3 (range, 0.10 to 6.39 cm^3), or 2.11% of the median rectum volume (range, 0.56% to 7.92%). The median $\text{Bladder}_{\text{overlap}}$ was 2.32 cm^3 (range, 0.31 to 11.36 cm^3), or 2.08% of the median bladder volume (range, 0.37% to 9.11%). The median percentage $\text{Rectum}_{\text{overlap}}$ of the training set was 2.16% (range, 0.95% to 7.92%), whereas that of the validation set was 2.11% (range, 0.56% to 5.33%). The median percentage $\text{Bladder}_{\text{overlap}}$ of the training set was 2.04% (range,

0.42% to 9.11%), whereas that of the validation set was 2.23% (range, 0.37% to 7.87%). Neither of these differences were statistically significant ($p = 0.94$ and $p = 0.86$, respectively). Pearson correlations between the boost plan $\text{Rectum}_{\text{overlap}}$ or $\text{Bladder}_{\text{overlap}}$ and dose-volumetric parameters are shown in Table 3. Of the parameters tested, there were statistically significant associations between $\text{Rectum}_{\text{overlap}}$ and Rectum V_{30} ($r = 0.728$, $p < 0.01$) and V_{20} ($r = 0.413$, $p < 0.01$). There were also statistically significant associations between $\text{Bladder}_{\text{overlap}}$ and Bladder V_{30} ($r = 0.901$, $p < 0.01$), V_{20} ($r = 0.623$, $p < 0.01$), and V_{10} ($r = 0.460$, $p < 0.01$). On linear regression analysis (Fig. 1C, D), the equation $[1.02 \times (\text{percentage Rectum}_{\text{overlap}}) + 3.51]$ predicts Rectum V_{30} with an R^2 of 0.53 ($p < 0.01$), and the equation $[1.25 \times (\text{percentage Bladder}_{\text{overlap}}) + 1.54]$ predicts Bladder V_{30} with an R^2 of 0.81 ($p < 0.01$), indicating that the full models accounts for 53% and 81% of data variability, respectively. The predictive abilities of the regression models for the boost plan were statistically indistinguishable between the training and

Table 3. Pearson product-moment correlations (*r*) associating the percentage overlap between the PTV and OARs (Rectum_{overlap} and Bladder_{overlap}, respectively) with dose-volumetric parameters for the boost plans

	Rectum _{overlap}		Bladder _{overlap}	
	<i>r</i>	p-value	<i>r</i>	p-value
Bladder				
V ₁₀	-0.237	0.13	0.460	<0.01
V ₂₀	-0.170	0.28	0.623	<0.01
V ₃₀	-0.116	0.47	0.901	<0.01
Rectum				
V ₁₀	0.231	0.14	-0.122	0.44
V ₂₀	0.413	<0.01	-0.160	0.31
V ₃₀	0.728	<0.01	-0.230	0.14
Femoral heads D _{mean}	0.155	0.33	0.144	0.36
PTV				
D _{min}	-0.207	0.19	0.004	0.98
D _{max}	0.250	0.11	0.234	0.14
Integral dose	-0.068	0.67	0.010	0.95
Conformity index	0.010	0.95	0.159	0.32
Gradient measure	0.085	0.59	0.065	0.68
Monitor units	0.140	0.38	-0.053	0.74

PTV, planning target volume; OARs, organs-at-risk.

validation sets, with $SR_{\text{Rectum}} = -0.28 \pm 1.94$ and $SR_{\text{Bladder}} = 0.28 \pm 1.40$ for the validation set (Fig. 2C, D).

According to the ROC method, the optimal cutoff value of boost Rectum_{overlap} to predict summation plan Rectum V₇₅ >15% was 3.5% (sensitivity 100%, specificity 94%, area under the curve [AUC] 0.974, 95% confidence interval [CI] 0.935 to 1.000, *p* < 0.01), and the optimal cutoff value of boost Rectum_{overlap} to predict Rectum V₇₅ >10% was 1.5% (sensitivity 83%, specificity 86%, AUC 0.905, 95% CI 0.831 to 0.980, *p* < 0.01). There were only two patients in our cohort with bladder V₈₀ >15%. However, the optimal cutoff value of boost Bladder_{overlap} to predict Bladder V₈₀ >10% was 5.0% (sensitivity 83%, specificity 100%, AUC 0.984, 95% CI 0.949 to 1.000, *p* < 0.01). Using our validation set of 28 additional patients, the three testing algorithms above appropriately categorized 93%, 86%, and 93% of patients, respectively.

Discussion and Conclusion

In prostate cancer radiotherapy, the degree of overlap between the rectum and PTV has been shown to be the most important predictor of benefit from IMRT as compared to 3D-CRT [1-

3], determines the limits of dose escalation possible [6,24], and can predict the degree of rectal sparing after hydrogel injection [18]. Similarly, in this study we have shown that the degree of overlap between PTV and bladder or rectum adversely effects sparing of that organ not only in the high-dose region of the dose-volume histogram, but also in the low-dose region as well. Although we speculated that the degree of overlap between PTV and OAR might affect other aspects of plan quality besides the dose to that OAR under our given set of optimization conditions, we found that the degree of overlap actually had minimal impact on the femoral head dose, integral dose, CI, GM, and MUs.

Several studies have also shown that the geometric relationship between PTV and OARs can be used to guide IMRT treatment planning. Some of the earliest reports of this were in the context of sparing the parotid glands in head and neck cancer [25-28], but more recently these methods have also been applied to prostate cancer [11-13]. Similarly, we have shown that the percentage overlap between PTV and bladder or rectum can be used to estimate rectal and bladder dose prior to optimization, and cutoff values for these overlap regions can be applied to accurately predict with a high sensitivity and specificity which plans are likely to deviate from the QUANTEC high-dose-region rectal and bladder dose-volume constraints. As such, whereas prior studies have been geared more towards treatment planning, the value of our study is that it provides a relatively simple front-end approach to guide "management" of the overlap region prior to optimization by identifying patients who are highly unlikely to achieve a dose-escalated treatment to the prostate while sparing OARs. This enables individualized, anatomy-specific guidance on the judicious use of additional measures to reduce the overlap volume prior to treatment planning. Furthermore, all of the above studies were carried out using IMRT, whereas our work extends similar principles to VMAT. It should be noted that the models generated in all of these studies (including our own) are dependent on the specific characteristics of the plan, prescription, and delivery, though our relatively common approach should be widely applicable (at least in principle) in clinical practices using VMAT.

There are several limitations to this study. First, this was a treatment planning system study only, and actual dose delivered from the generated plans was not measured. As such, toxicity data is not available, though this has been reported previously [29,30]. Another limitation to the concept of using the PTV-OAR overlap to stratify patients is that it is

not meaningful when the OAR and target do not overlap (but are merely close to overlapping), thus having the potential to oversimplify the relative spatial configuration of the PTV and OAR. As described by Wu et al. [27], while the more complex overlap volume histogram method would resolve much of this issue, we would contend that looking at the overlap alone provides a sufficient amount of information in a disease like prostate cancer, in which the PTV for both the primary and boost plans will overlap bladder and rectum to varying extents in virtually all patients when using the RTOG-recommended 5 to 15 mm margins around the prostate. Moore et al. [13] also confirmed that relying on the overlap volume as a geometric indicator was a straightforward and sufficient means of developing a prostate cancer IMRT quality control tool.

In this study, we have shown that the overlap between PTV and bladder or rectum adversely affects sparing of that organ. Regression equations can be applied to the percentage overlap volume to accurately predict the ability of VMAT planning to achieve high-dose region constraints for a given OAR in the primary and boost plans, and a percentage overlap between the boost plan PTV and rectum greater than 3.5% of the total rectal volume was highly predictive of a plan with a Rectum V_{75} exceeding the QUANTEC constraint of 15%. This information has the potential to enable clinicians to tailor technology and treatment decisions in a patient-specific manner based on the anatomy of the patient.

Conflict of Interest

No potential conflict of interest relevant to this article was reported.

References

1. Corletto D, Iori M, Paiusco M, et al. Inverse and forward optimization of one- and two-dimensional intensity-modulated radiation therapy-based treatment of concave-shaped planning target volumes: the case of prostate cancer. *Radiother Oncol* 2003;66:185-95.
2. Damen EM, Brugmans MJ, van der Horst A, et al. Planning, computer optimization, and dosimetric verification of a segmented irradiation technique for prostate cancer. *Int J Radiat Oncol Biol Phys* 2001;49:1183-95.
3. De Meerleer GO, Vakaet LA, De Gerssem WR, De Wagter C, De Naeyer B, De Neve W. Radiotherapy of prostate cancer with or without intensity modulated beams: a planning comparison. *Int J Radiat Oncol Biol Phys* 2000;47:639-48.
4. Wolff D, Stieler F, Welzel G, et al. Volumetric modulated arc therapy (VMAT) vs. serial tomotherapy, step-and-shoot IMRT and 3D-conformal RT for treatment of prostate cancer. *Radiother Oncol* 2009;93:226-33.
5. Cozzi L, Dinshaw KA, Shrivastava SK, et al. A treatment planning study comparing volumetric arc modulation with RapidArc and fixed field IMRT for cervix uteri radiotherapy. *Radiother Oncol* 2008;89:180-91.
6. Goulet CC, Herman MG, Hillman DW, Davis BJ. Estimated limits of IMRT dose escalation using varied planning target volume margins. *Phys Med Biol* 2008;53:3777-88.
7. Chen ME, Johnston DA, Tang K, Babaian RJ, Troncso P. Detailed mapping of prostate carcinoma foci: biopsy strategy implications. *Cancer* 2000;89:1800-9.
8. Epstein JI, Walsh PC, Carmichael M, Brendler CB. Pathologic and clinical findings to predict tumor extent of nonpalpable (stage T1c) prostate cancer. *JAMA* 1994;271:368-74.
9. Kassim I, Dirks ML, Heijmen BJ. Evaluation of the dosimetric impact of non-exclusion of the rectum from the boost PTV in IMRT treatment plans for prostate cancer patients. *Radiother Oncol* 2009;92:62-7.
10. Zelefsky MJ, Fuks Z, Happersett L, et al. Clinical experience with intensity modulated radiation therapy (IMRT) in prostate cancer. *Radiother Oncol* 2000;55:241-9.
11. Zhu X, Ge Y, Li T, Thongphiew D, Yin FF, Wu QJ. A planning quality evaluation tool for prostate adaptive IMRT based on machine learning. *Med Phys* 2011;38:719-26.
12. Appenzoller LM, Michalski JM, Thorstad WL, Mutic S, Moore KL. Predicting dose-volume histograms for organs-at-risk in IMRT planning. *Med Phys* 2012;39:7446-61.
13. Moore KL, Brame RS, Low DA, Mutic S. Experience-based quality control of clinical intensity-modulated radiotherapy planning. *Int J Radiat Oncol Biol Phys* 2011;81:545-51.
14. Zelefsky MJ, Harrison A. Neoadjuvant androgen ablation prior to radiotherapy for prostate cancer: reducing the potential morbidity of therapy. *Urology* 1997;49(3A Suppl):38-45.
15. Gauthier I, Carrier JF, Beliveau-Nadeau D, Fortin B, Tausky D. Dosimetric impact and theoretical clinical benefits of fiducial markers for dose escalated prostate cancer radiation treatment. *Int J Radiat Oncol Biol Phys* 2009;74:1128-33.
16. Azcona JD, Li R, Mok E, Hancock S, Xing L. Automatic prostate tracking and motion assessment in volumetric modulated arc therapy with an electronic portal imaging device. *Int J Radiat Oncol Biol Phys* 2013;86:762-8.
17. Das S, Liu T, Jani AB, et al. Comparison of image-guided radiotherapy technologies for prostate cancer. *Am J Clin Oncol* 2013 Feb 20 [Epub]. <http://dx.doi.org/10.1097/COC.0b013e31827e4eb9>.
18. Yang Y, Ford EC, Wu B, et al. An overlap-volume-histogram based method for rectal dose prediction and automated treatment planning in the external beam prostate radiotherapy

- following hydrogel injection. *Med Phys* 2013;40:011709.
19. Susil RC, McNutt TR, DeWeese TL, Song D. Effects of prostate-rectum separation on rectal dose from external beam radiotherapy. *Int J Radiat Oncol Biol Phys* 2010;76:1251-8.
 20. Pinkawa M, Corral NE, Caffaro M, et al. Application of a spacer gel to optimize three-dimensional conformal and intensity modulated radiotherapy for prostate cancer. *Radiother Oncol* 2011;100:436-41.
 21. Marks LB, Yorke ED, Jackson A, et al. Use of normal tissue complication probability models in the clinic. *Int J Radiat Oncol Biol Phys* 2010;76(3 Suppl):S10-9.
 22. Breitman K, Rathee S, Newcomb C, et al. Experimental validation of the Eclipse AAA algorithm. *J Appl Clin Med Phys* 2007;8:76-92.
 23. Rodgers JL, Nicewander AW. Thirteen ways to look at the correlation coefficient. *Am Stat* 1988;42:59-66.
 24. Mohan R, Wang X, Jackson A, et al. The potential and limitations of the inverse radiotherapy technique. *Radiother Oncol* 1994;32:232-48.
 25. Hunt MA, Jackson A, Narayana A, Lee N. Geometric factors influencing dosimetric sparing of the parotid glands using IMRT. *Int J Radiat Oncol Biol Phys* 2006;66:296-304.
 26. Vineberg KA, Eisbruch A, Coselmon MM, McShan DL, Kessler ML, Fraass BA. Is uniform target dose possible in IMRT plans in the head and neck? *Int J Radiat Oncol Biol Phys* 2002;52:1159-72.
 27. Wu B, Ricchetti F, Sanguineti G, et al. Patient geometry-driven information retrieval for IMRT treatment plan quality control. *Med Phys* 2009;36:5497-505.
 28. Wu B, McNutt T, Zahurak M, et al. Fully automated simultaneous integrated boosted-intensity modulated radiation therapy treatment planning is feasible for head-and-neck cancer: a prospective clinical study. *Int J Radiat Oncol Biol Phys* 2012;84:e647-53.
 29. Cheung MR, Tucker SL, Dong L, et al. Investigation of bladder dose and volume factors influencing late urinary toxicity after external beam radiotherapy for prostate cancer. *Int J Radiat Oncol Biol Phys* 2007;67:1059-65.
 30. Michalski JM, Gay H, Jackson A, Tucker SL, Deasy JO. Radiation dose-volume effects in radiation-induced rectal injury. *Int J Radiat Oncol Biol Phys* 2010;76(3 Suppl):S123-9.